Bender-Wu branch points in the cubic oscillator

1995 J. Phys. A: Math. Gen. 28 4589

(http://iopscience.iop.org/0305-4470/28/16/016)

J. Phys. A: Math. Gen. 27 (1995) 4589–4598. Printed in the UK

Bender–Wu branch points in the cubic oscillator

Gabriel Alvarez

Departamento de Física Teórica, Facultad de Ciencias Físicas Universidad Complutense, 28040 Madrid, Spain

Received 20 March 1995

Abstract. The analytic continuation of the resonances of the cubic anharmonic oscillator to complex values of the coupling constant is studied with semiclassical and numerical methods. Bender–Wu branch points, at which level crossing occurs, are calculated and labelled by a process of analytic continuation. The different resonances are the values that a single analytic function takes on different sheets of a Riemann surface whose topology is described.

1. Introduction

In their famous 1969 paper [1], Bender and Wu studied the analytic continuation of the eigenvalues of the quartic anharmonic oscillator to complex values of the coupling constant. One of their most noteworthy results was that the energy levels have an infinite number of branch points at which level crossing occurs. Bender and Wu obtained asymptotic formulae for the positions of these branch points, and performed numerical calculations of the associated eigenvalues to describe the analytic configuration of the corresponding Riemann surface. This paper was closely followed by another in which Simon [2] gave rigorous proofs of many of the properties discussed by Bender and Wu, and extended their results to some multidimensional coupled anharmonic oscillators.

Bender–Wu branch points are not a peculiarity of the quartic anharmonic oscillator, and among the several models which have been studied [3–9] one can find rigorous results for general periodic potentials [5], explicit solutions for delta-function perturbations of a square well [8], and polynomial potentials for which a finite number of eigenfunctions can be explicitly calculated (the so-called 'quasi-integrable' systems [9]).

New interest in the subject arose when Benassi *et al* [10] realized the role played by Bender–Wu branch points in the asymptotic behaviour at large external electric fields of the resonances of the LoSurdo–Stark Hamiltonian for atomic hydrogen. The corresponding Schrödinger equation is separable in parabolic coordinates, and each separated equation is equivalent to a two-dimensional isotropic quartic anharmonic oscillator. Benassi *et al* determined the high-field asymptotics of a resonance thought to come from the ground state, and suggested that for excited states the asymptotic behaviour would be determined by a similar formula, whose validity would depend on the number of Bender–Wu branch cuts crossed by the separation constants as the electric field increased from zero to infinity. Benassi and Grecchi [11] plotted these trajectories for the ground state and one excited state but, lacking a method to calculate the positions of the branch points, they could only conjecture qualitatively the locations of the cuts for their formula to be valid.

A few years later, Shanley [12] addressed the original problem of calculating accurately the branch points of the one-dimensional quartic anharmonic oscillator. He used an iterative

0305-4470/95/164589+10$19.50

procedure based on a tenth-order Adams–Moulton numerical integration of the Schrödinger equation, succeeded in locating to seven-digit accuracy some branch points, and pointed out an inconsistency in the assignment that Bender and Wu made of what levels cross at each branch point (which in turn determines the topology of the associated Riemann surface).

Most recently, in the context of the LoSurdo–Stark effect, Alvarez and Silverstone [13] found a simple iterative algorithm to calculate numerically the position of the Bender–Wu branch points to arbitrary precision, and gave a detailed picture of their role in the LoSurdo–Stark effect, following the separation constants and resonance eigenvalues as the electric field increases from zero to infinity. The analytic configuration of the Riemann surface was clarified and asymptotic expansions for the separation constants and eigenvalues as the electric field tends to infinity were obtained.

In this paper, the same numerical and semiclassical methods are applied to study the analytic configuration of the eigenvalues of the cubic anharmonic oscillator, a standard textbook example of perturbation theory which, for purely imaginary values of the coupling constant, describes the universal properties of the Lee–Yang edge singularity of the Ising model [14–16]. Complex eigenvalues (resonances) of the cubic anharmonic oscillator for real values of the coupling constant were first calculated numerically by Yaris *et al* [17], who emphasized the empirical validity of complex dilation even for this non-dilation-analytic potential, gave the first term of the Rayleigh–Schrödinger perturbation series and the (exponentially small) asymptotic behaviour of the imaginary part of these eigenvalues as the coupling constant tends to zero along the real axis. These results were extended by Alvarez [18, 19], who also found the asymptotic behaviour of the eigenvalues for large values of the coupling constant. In section 2 of the present paper we briefly review the definition and characterization of resonances, the consequences of Symanzik scaling and the large coupling-constant behaviour. Section 3 is dedicated to the numerical calculation of the branch points, at which level crossing occurs. The different resonances turn out to be the values that a single analytic function takes on different sheets of a Riemann surface. The structure of this surface is determined by the pattern of crossings (i.e. the labelling of the branch points) which is identified by analytic continuation. Section 4 is dedicated to the small coupling-constant behaviour of the resonances, in particular when the coupling constant tends to zero crossing an infinite number of branch cuts. The paper ends with a brief summary.

2. Resonances of the cubic anharmonic oscillator

Physical intuition suggests that when the coupling constant g is positive, the cubic anharmonic oscillator Hamiltonian,

$$H = \tfrac{1}{2}p^2 + \tfrac{1}{2}kx^2 + gx^3 \tag{1}$$

does not have bound states but resonances: the particle, initially confined in the potential well, will escape to $x = -\infty$ by tunnelling. This apparently simple Hamiltonian poses, however, a mathematically complicated problem, since the minimal operator generated by the action of the formal expression (1) on the space of infinitely-differentiable functions of compact support admits infinitely many self-adjoint extensions (see, for example, [20]), and there is no physical criterion to single one of them out. This is the quantum analogue of the fact that a classical particle initially moving in $(-\infty, -1/2g)$ reaches $x = -\infty$ in a finite amount of time. Nevertheless, Caliceti *et al* [21] showed that if the coupling constant g is complex and $\operatorname{Im} g > 0$, the operator (1) has non-empty discrete spectrum (i.e. isolated eigenvalues of finite multiplicity) and the analytic continuation of these eigenvalues across

the real axis is not single valued. The global properties of this analytic continuation are conveniently studied characterizing the resonances by boundary conditions in appropriate sectors of the complex plane. If $g \neq 0$, the differential equation

$$\left(-\frac{1}{2}\frac{d^2}{dx^2}+\frac{k}{2}x^2+gx^3\right)\psi(x)=E(k,g)\psi(x) \tag{2}$$

has a unique solution (up to a multiplicative constant) $\psi_+(x)$ with asymptotic behaviour dominated by

$$\psi_+(x) \sim \exp(-\tfrac{2}{5}g^{1/2}x^{5/2}) \tag{3}$$

as $x \to \infty$ in the sector

$$0 < \tfrac{1}{2}\arg(g)+\tfrac{5}{2}\arg(x) < \pi. \tag{4}$$

Similarly, there exists a solution with asymptotic behaviour dominated by

$$\psi_-(x) \sim \exp(-\tfrac{2}{5}g^{1/2}(-x)^{5/2}) \tag{5}$$

as $(-x) \to \infty$ in the sector

$$-\tfrac{1}{2}\pi < \tfrac{1}{2}\arg(g)+\tfrac{5}{2}\arg(x) < \tfrac{1}{2}\pi. \tag{6}$$

The complex number $E(k, g)$ is a resonance eigenvalue if there exists a solution $\psi(x)$ (the resonance eigenvector) of the differential equation (2) for which both asymptotic boundary conditions (3) and (5) hold in the common subsector

$$0 < \tfrac{1}{2}\arg(g)+\tfrac{5}{2}\arg x < \tfrac{1}{2}\pi. \tag{7}$$

For example, one can imagine that the differential equation (2) is integrated along the rays $\arg(\pm x) = \pi/10 - \arg(g)/5$, which lie halfway in the sector of convergence given by equation (7).

A key property of the resonances follows from the change of variable $x \to \lambda x$:

$$E(k, g) = \lambda^{-2}E(\lambda^4 k, \lambda^5 g). \tag{8}$$

Equation (8) is usually known as Symanzik scaling [2]. For $\lambda = e^{i\pi}$, it shows that

$$E(k, g) = E(k, ge^{i5\pi}) \tag{9}$$

that is to say, there is a global $\frac{2}{5}$ singularity at the origin (in the sense defined by Simon [2]) with 'two and a half' Riemann sheets, and for $\lambda = e^{i\pi/2}$ one obtains

$$E(k, g) = e^{-i\pi}E(k, ge^{i5\pi/2}). \tag{10}$$

Furthermore, since $\lambda = k^{-1/4}$ scales out the harmonic constant k, hereafter we will consider only

$$E(g) \equiv E(1, g). \tag{11}$$

With an argument based on Borel summability, Caliceti *et al* [21] showed that for $\arg(g) = \pi/2$, the resonances are real. A slightly more general statement is

$$E(|g|e^{i\arg(g)}) = E(|g|e^{i\pi}e^{-i\arg(g)})^* \tag{12}$$

where the asterisk denotes complex conjugation and the arguments have to be understood modulo 5π. In particular, for $\arg(g) = \pi/2$ and 3π the resonances are real, and using equation (10) it can be checked that for $\arg(g) = 7\pi/4$ and $17\pi/4$ the resonances are purely imaginary.

It is easy to find also an explicit formula for the large coupling-constant behaviour of the resonances [18], which follows from the application of Dunham's condition [22] to a

path enclosing the two transition points $x_1 \sim (E/g)^{1/3}$ and $x_2 \sim (E/g)^{1/3}e^{-i2\pi/3}$ in the appropriate sectors of the complex plane:

$$E_n(g) \sim \frac{1}{2}\left(\frac{5\pi^{3/2}(2n+1)}{\sqrt{3}\Gamma(1/3)\Gamma(1/6)}\right)^{6/5}(2ge^{-i\pi/2})^{2/5} \text{ as } g \to \infty \tag{13}$$

where $n = 0, 1, 2, \ldots$ is the usual harmonic oscillator quantum number.

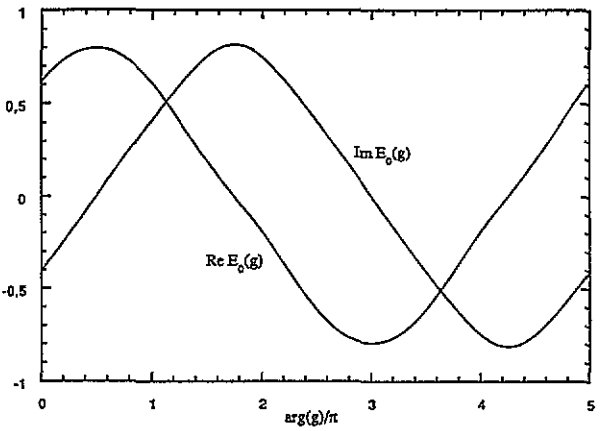

Figure 1. Real and imaginary parts of the $n = 0$ resonance as a function of the argument of the coupling constant g for a fixed value of $|g| = 1$.

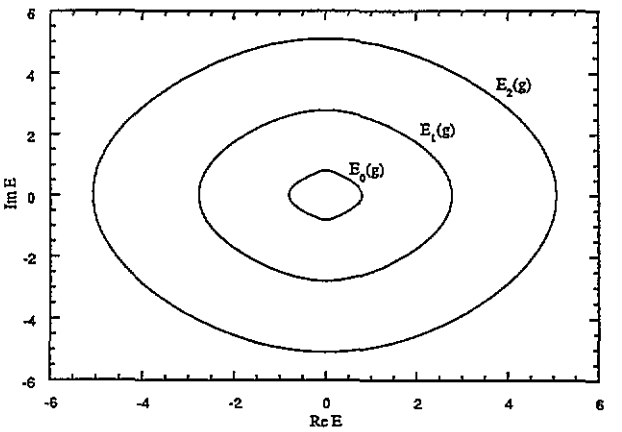

Figure 2. Path in the complex E plane of the $n = 0$, 1 and 2 resonances for $g = e^{i\arg(g)}$, $\arg(g) \in [0, 5\pi]$.

All this information is illustrated in figures 1 and 2. The resonance eigenvalues have been calculated by expansion of the resonance eigenvectors in a set of square-integrable functions along a ray lying halfway in the sector of convergence. Figure 1 shows both Re E and Im E for the $n = 0$ resonance as a function of $\arg(g)$ for a fixed value of $|g| = 1$, while figure 2 shows the path in the complex E plane of the $n = 0$, 1, and 2 resonances for $g = e^{i\arg(g)}$, $\arg(g) \in [0, 5\pi]$.

3. Bender–Wu branch points

Equation (13) and figure 2 show that for fixed large $|g|$, the resonances describe concentric, non-intersecting (asymptotically) circular paths as $\arg(g)$ increases from 0 to 5π. When $|g|$ decreases, these paths are progressively distorted until, for certain values of g, they cross. There are several equivalent analytic characterizations of these branch points [2]. For example,

$$\int_\gamma \psi(x)^2\,\mathrm{d}x = 0 \tag{14}$$

where γ denotes the above-mentioned integration path (note that the integrand is the square of the resonance wavefunction, not the modulus squared), or the fact that the derivative of the resonance energy with respect to the coupling constant becomes infinite at the branch point (see again [2]). From a calculational point of view it is most convenient to take advantage of the square-root nature of the branch points. Suppose one such crossing occurs at g_c, and denote by $E_+(g)$ and $E_-(g)$ the two eigenvalues involved in the crossing, i.e. the two branches of a Puiseaux series in a neighbourhood of g_c:

$$E_\pm(g) = E(g_c) \pm a_{1/2}(g-g_c)^{1/2} + \cdots. \tag{15}$$

Pick two initial values g_1 and g_2 close to the branch point g_c, and note that

$$\frac{E_+(g_1)-E_-(g_1)}{E_+(g_2)-E_-(g_2)} \approx \frac{(g_1-g_c)^{1/2}}{(g_2-g_c)^{1/2}}. \tag{16}$$

The form of the solution for g_c in the previous equation suggests the following iterative algorithm: For $i = 1, 2, \ldots$,

$$Q_{i+1} = \left[\frac{E_+(g_i)-E_-(g_i)}{E_+(g_{i+1})-E_-(g_{i+1})}\right]^2 \tag{17}$$

$$g_{i+2} = \frac{g_i - g_{i+1}Q_{i+1}}{1-Q_{i+1}}. \tag{18}$$

The eigenvalues $E_+(g)$ and $E_-(g)$ can be easily calculated by the expansion in square-integrable functions mentioned above, and the algorithm of equations (17) and (18) converges without difficulty in typically ten iterations. To understand the structure of the associated Riemman surface, let us consider first a group of branch points centred around $\arg(g) = 9\pi/8$ with arguments extending symmetrically by up to $\pm\pi/8$ around this ray. The 'lowest' branch points of this group are shown in table 1. Note that the algorithm described by equations (17) and (18) gives only the position g_c and eigenvalue $E(g_c)$ of each branch point. What does not come out directly of the algorithm is the fact that each branch point can be uniquely labelled by a pair of different non-negative integers, n_1 and n_2, which identify the unperturbed levels involved in the crossing. This assignment requires a series of numerical calculations in which the coupling constant starts at $g = 0$, where each eigenvalue can be labelled by its harmonic oscillator quantum number $E_n = (n+\frac{1}{2})$, then traces a path in the complex g plane encircling just one branch point, and returns to the origin. One such path is shown in figure 3(*a*). It turns out that each level, followed by continuity, returns to its initial value, except two of them which are exchanged and provide the labelling of the branch point, as can be seen in the example of figure 3. Furthermore, for each pair of different quantum numbers there is exactly one branch point (with $\pi < \arg(g_{n_1 n_2}) < 5\pi/4$) that exchanges them. Once this classification scheme is known, it is possible to mimic the

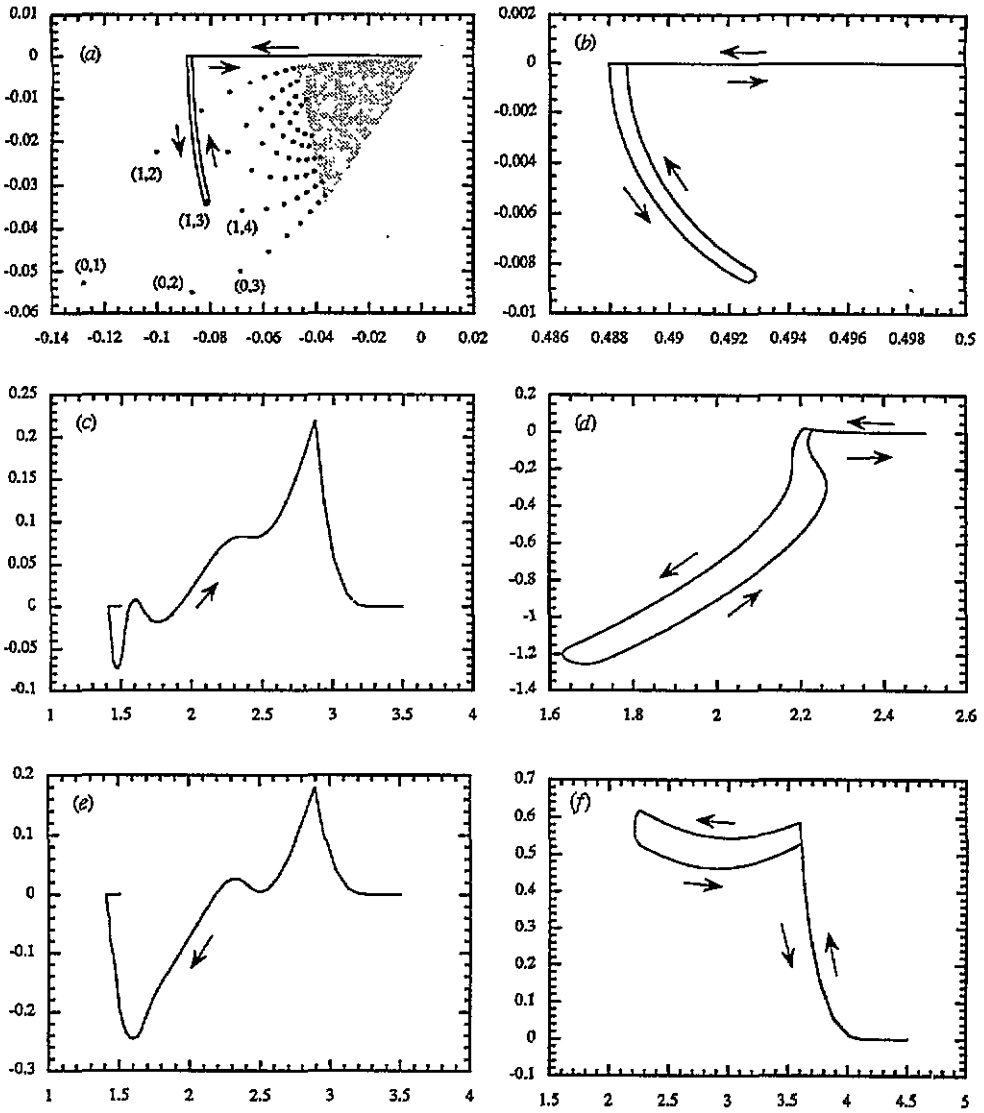

Figure 3. (*a*) Path in the complex g plane starting at the origin and encircling just one of the branch points; (*b*)–(*f*) Corresponding paths in the complex E plane for the $n = 0$ to $n = 4$ resonances.

calculation of Bender and Wu in [1] for the asymptotic evaluation of equation (14) and obtain the following formula for the position of the branch points:

$$\frac{1}{54g_{n_1n_2}^2} \sim \left(n_2 + \frac{1}{2}\right) - \mathrm{i}\left(n_1 + \frac{1}{2}\right). \tag{19}$$

The validity of this equation is illustrated in figure 4.

Let us consider now the overall distribution of branch points. Besides those with $\pi < \arg(g_{n_1n_2}) < 5\pi/4$, the symmetry properties of the eigenvalues given by equations (9), (10) and (12) imply the existence of another three equivalent families of branch points centred around $19\pi/8$, $29\pi/8$ and $39\pi/8$ respectively, with arguments extending again

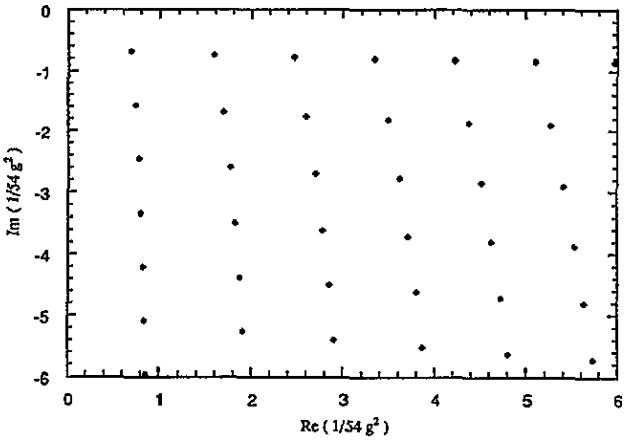

Figure 4. Branch points of the cubic anharmonic oscillator with $\pi < \arg(g) < 5\pi/4$.

Table 1. Branch points of the cubic anharmonic oscillator with $0 \leqslant n_1 < n_2 \leqslant 5$ and $\pi < \arg(g_{n_1 n_2}) < 5\pi/4$.

n_1	n_2	$\lvert g_{n_1 n_2}\rvert$	$\arg(g_{n_1 n_2})$	$\mathrm{Re}\, E_{n_1 n_2}$	$-\mathrm{Im}\, E_{n_1 n_2}$
0	1	0.138 095 904 611 6579	3.534 291 735 288 5174	0.614 395 336	0.072 245 524
0	2	0.102 869 748 100 2435	3.706 271 074 037 8341	0.620 728 761	0.049 472 828
0	3	0.084 633 451 129 7112	3.773 037 003 918 1804	0.618 915 136	0.039 571 861
0	4	0.073 394 335 327 6270	3.808 243 510 665 8928	0.616 567 624	0.034 130 938
0	5	0.065 642 745 448 3712	3.830 021 024 062 1947	0.614 450 301	0.030 664 771
1	2	0.102 869 748 100 2435	3.362 312 396 539 2006	1.532 741 868	0.126 931 361
1	3	0.087 950 489 301 7066	3.534 291 735 288 5174	1.584 122 784	0.108 712 578
1	4	0.076 739 806 056 5118	3.628 195 462 099 9905	1.602 306 092	0.090 093 150
1	5	0.068 544 918 309 3794	3.685 972 477 666 7937	1.609 648 472	0.076 752 009
2	3	0.084 633 451 129 7112	3.295 546 466 658 8544	2.424 204 411	0.164 619 861
2	4	0.076 739 806 056 5118	3.440 388 008 477 0443	2.509 524 184	0.167 008 230
2	5	0.069 611 976 772 7027	3.534 291 735 288 5174	2.552 425 738	0.149 810 471
3	4	0.073 394 335 327 6270	3.260 339 959 911 1419	3.307 175 834	0.192 238 778
3	5	0.068 544 918 309 3794	3.382 610 992 910 2411	3.415 577 488	0.217 546 307
4	5	0.065 642 745 448 3712	3.238 562 446 514 8401	4.186 432 156	0.213 822 351

symmetrically by up to $\pm\pi/8$. In particular π and 5π, i.e. the real axis, is a limit of arguments of singularities (hence the multivaluedness of the analytic continuation across this axis realized by Caliceti *et al* [21]). Branch cuts can be drawn between corresponding pairs of branch points, and the Riemann surface can be described as an infinite number of 'two and a half' sheets joined to each other at exactly four branch points, with a global $\frac{2}{5}$ singularity at the origin, which is a limit point of the four families of branch points.

4. Small coupling-constant asymptotics

To study the small coupling-constant asymptotics let us introduce the new variable $z = gx + \frac{1}{6}$. The differential equation is now

$$-\tfrac{1}{2}g^4 w'' + (z^3 - \tfrac{1}{12}z - g^2 E + \tfrac{1}{108})w = 0 \tag{20}$$

and the sector of convergence is

$$0 < \arg(z) - \tfrac{4}{5}\arg(g) < \tfrac{1}{5}\pi. \tag{21}$$

This particular scaling fixes the zeroth-order turning points and allows some additional symmetry features to be understood. For example, if $\arg(g) = \pi/2$ one can take $\arg(z) = \pi/2$ and the differential equation becomes

$$-\tfrac{1}{2}|g|^4 w'' + \mathrm{i}(-x^3 + \tfrac{1}{12}x - g^2E + \tfrac{1}{108})w = 0 \tag{22}$$

with x real. Since the eigenvalues are real, one obtains

$$\mathrm{Re}(g^2E) = \tfrac{1}{108}. \tag{23}$$

Similarly, if $\arg(g) = 9\pi/8$, that is to say, in the bisector of the first family of branch points, one can take $\arg(z) = \pi$, the differential equation has the same structure as equation (22) with i replaced by $-\mathrm{i}$, and equation (23) still holds (e.g., $g_{n,2n+1}$ in table 1).

The asymptotic behaviour can be obtained via the relation between the Rayleigh–Schrödinger perturbation theory and the Jeffreys–Wentzel–Kramers–Brillouin (JWKB) series [19, 23], i.e. the perturbation series will be generated using the JWKB with g^2 playing the role of $\hbar$. The wavefunction w is expanded as a JWKB series in g^2,

$$w = \exp\left(\frac{1}{g^2}\int S\,\mathrm{d}z\right) \tag{24}$$

$$S = \sum_{N=0}^{\infty} g^{2N} S^{(N)}(z) \tag{25}$$

where the JWKB function $S(z)$ satisfies a Riccati equation

$$\tfrac{1}{2}S(z)^2 + \tfrac{1}{2}g^2 S'(z) - p(z) = 0 \tag{26}$$

which can be recursively solved for the $S^{(N)}$. The quantization condition is given by Dunham's formula [22]

$$\frac{1}{2\pi\mathrm{i}}\oint_{\Gamma} S\,\mathrm{d}z = ng^2 \tag{27}$$

where Γ is a path enclosing the two turning points in the appropriate sectors of the complex plane (the third turning point gives an exponentially small contribution). Details of the calculation to high order can be seen in [18, 19] and will be omitted; for the moment it is enough to consider the second-order quantization formula,

$$\frac{1}{2\pi\mathrm{i}}\oint_{\Gamma} \sqrt{2(z-z_+)(z-z_-)(z-z_0)}\,\mathrm{d}z \sim (n+\tfrac{1}{2})g^2 \tag{28}$$

where the integration can be explicitly performed to give

$$\frac{1}{4\sqrt{2}}(z_+ - z_-)^2(z_+ - z_0)^{1/2}\,{}_2\mathrm{F}_1\left(-\frac{1}{2}, \frac{3}{2}; 3; \frac{z_+ - z_-}{z_+ - z_0}\right) \sim \left(n + \frac{1}{2}\right)g^2. \tag{29}$$

The turning points z_0 and $z_\pm$ are the roots of the polynomial

$$p(z) = z^3 - \tfrac{1}{12}z - g^2E + \tfrac{1}{108} \tag{30}$$

which can be written in terms of Gauss hypergeometric ${}_2\mathrm{F}_1$ function:

$$z_0 = -\tfrac{1}{3}\,{}_2\mathrm{F}_1(\tfrac{1}{3}, -\tfrac{1}{3}; \tfrac{1}{2}; 54g^2E) \tag{31}$$

$$z_\pm = -\tfrac{1}{2}z_0 + (2g^2E)^{1/2}\,{}_2\mathrm{F}_1(\tfrac{1}{6}, \tfrac{5}{6}; \tfrac{3}{2}; 54g^2E). \tag{32}$$

The last step is to perform the appropriate expansions in the small coupling-constant limit $g \to 0$. There are two different regimes, corresponding to the two distinguished values $g^2E = 0$ and $g^2E = 1/54$ for which the polynomial $p(z)$ has a double root.

The lowest-order term of the expansion of equation (29) around $g^2E = 0$ is

$$g^2E_n(g) \sim (n + \tfrac{1}{2})g^2 \tag{33}$$

or

$$E_n(g) \sim (n + \tfrac{1}{2}) \tag{34}$$

the first term of the usual Rayleigh–Schrödinger series. This expansion is asymptotic to the eigenvalues for $0 < \arg(g) < \pi$ independently of the eigenvalue, and even in a certain region beyond $\arg(g) = \pi$ for each particular eigenvalue, as can be seen from the positions of the branch points; for example, the results of figure 3(*b*) for $E_0(g)$ can be accounted for with second-order perturbation theory. As mentioned above, higher-order terms can be readily obtained and are tabulated in [19]. For later comparison, the following equation shows the structure of the asymptotic series up to terms in g^4:

$$E_n(g) \sim (n + \tfrac{1}{2}) - [\tfrac{15}{4}(n + \tfrac{1}{2})^2 + \tfrac{7}{16}]g^2 - [\tfrac{11\,280}{256}(n + \tfrac{1}{2})^3 + \tfrac{4620}{256}(n + \tfrac{1}{2})]g^4 - \cdots. \tag{35}$$

Consider now the expansion of equation (29) around the second value $g^2E = 1/54$, which to lowest order yields

$$\mathrm{i}(-g^2E_n(g) + \tfrac{1}{54}) \sim (n + \tfrac{1}{2})g^2 \tag{36}$$

or

$$E_n(g) \sim \frac{1}{54g^2} + \mathrm{i}\left(n + \frac{1}{2}\right). \tag{37}$$

This expansion is asymptotic to the eigenvalues for $5\pi/4 < \arg(g) < 9\pi/4$ independently of the eigenvalue, and in a larger region for each particular eigenvalue. Again, higher-order terms can be easily calculated and the result to order g^4 is

$$E_n(g) \sim \frac{1}{54g^2} + \mathrm{i}(n + \tfrac{1}{2}) - [\tfrac{15}{4}(n + \tfrac{1}{2})^2 + \tfrac{7}{16}]g^2 + \mathrm{i}[\tfrac{11\,280}{256}(n + \tfrac{1}{2})^3 + \tfrac{4620}{256}(n + \tfrac{1}{2})]g^4 - \cdots. \tag{38}$$

Finally, to illustrate these results consider the path of figure 5(*a*), in which the coupling constant g starts upwards along the ray $\arg(g) = \pi/2$, then traces counterclockwise an arc of circle to $\arg(g) = 3\pi/2$ and finally returns to the origin along this ray. This path encloses all the branch points of the first family, and its initial and final portions are in the regions of validity of equations (35) and (38) respectively. In figure 5(*b*), the markers correspond to (exact) numerical calculations of the $n = 1$ resonance along the path, while the lines correspond to the results given by the asymptotic formulae (the $n = 1$ resonance has been chosen as an example because the relevant features of the plot can be seen in the same scale; similar results are obtained for the other resonances).

5. Summary

The resonances of the cubic anharmonic oscillator are the values that a single analytic function takes on different sheets of a Riemann surface. This surface consists of an infinite number of 'two and a half' sheets joined to each other at exactly four square-root branch points. The origin, which globally behaves as a $\frac{2}{5}$ singularity, is a limit point of the four families of branch points. Semiclassical formulae and efficient numerical algorithms have

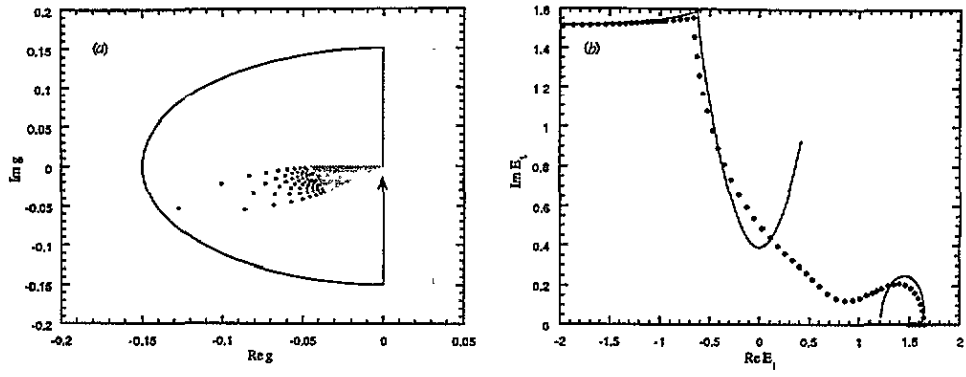

Figure 5. (*a*) Path in the complex g plane enclosing all the branch points with $\pi < \arg(g) < 5\pi/4$; (*b*) the markers correspond to numerical calculations of $E_1(g)$ along the path (*a*); the lines correspond to the results given by suitable asymptotic expansions discussed in the text.

been developed to locate the branch points, and a process of numerical analytic continuation has permitted the identification of what levels cross at each branch point, which in turn is a description of the topology of the Riemann surface. Finally, a JWKB expansion provides a unified derivation of the asymptotic behaviour of the resonances as the coupling constant tends to zero in different regions of the Riemann surface. These results have been checked against exact numerical calculations.

References

[1] Bender C M and Wu T T 1969 *Phys. Rev.* **184** 1231
[2] Simon B 1970 *Ann. Phys., NY* **58** 76
[3] Blanch G and Glemm D S 1969 *Math. Comput.* **23** 97
[4] Bender C M, Happ H J and Svetitsky B 1974 *Phys. Rev.* D **9** 2324
[5] Avron J E and Simon B 1978 *Ann. Phys., NY* **110** 85
[6] Hunter C and Guerrieri B 1981 *Stud. Appl. Math.* **64** 113
[7] Hunter C and Guerrieri B 1982 *Stud. Appl. Math.* **66** 217
[8] Ushveridze A G 1988 *J. Phys. A: Math. Gen.* **21** 955
[9] Turbiner A V and Ushveridze A G 1987 *Phys. Lett.* **126A** 181
[10] Benassi L, Grecchi V, Harrell E and Simon B 1979 *Phys. Rev. Lett.* **42** 704
[11] Benassi L and Grecchi V 1980 *J. Phys. B: At. Mol. Phys.* **13** 911
[12] Shanley P E 1988 *Phys. Lett.* **117A** 161
[13] Alvarez G and Silverstone H J 1994 *Phys. Rev.* A **50** 4679
[14] Yang C N and Lee T D 1952 *Phys. Rev.* **87** 404
[15] Lee T D and Yang C N 1952 *Phys. Rev.* **87** 410
[16] Fisher M E 1978 *Phys. Rev. Lett.* **40** 1610
[17] Yaris R, Bendler J, Lovett R A, Bender C M and Fedders P A 1978 *Phys. Rev.* A **18** 1816
[18] Alvarez G 1988 *Phys. Rev.* A **37** 4079
[19] Alvarez G 1989 *J. Phys. A: Math. Gen.* **22** 617
[20] Naimark N A 1964 *Linear Differential Operators II* (London: Harrap)
[21] Caliceti E, Graffi S and Maioli M 1980 *Commun. Math. Phys.* **75** 51
[22] Dunham J L 1932 *Phys. Rev.* **41** 713
[23] Alvarez G, Graffi S and Silverstone H J 1988 *Phys. Rev.* A **38** 1687